

Evidence from the Very Long Baseline Array that J1502SE/SW are Double Hotspots, not a Supermassive Binary Black Hole

J. M. Wrobel^{1,2}, R. C. Walker¹, and H. Fu³

ABSTRACT

SDSS J150243.09+111557.3 is a merging system at $z = 0.39$ that hosts two confirmed AGN, one unobscured and one dust-obscured, offset by several kiloparsecs. Deane et al. recently reported evidence from the European VLBI Network (EVN) that the dust-obscured AGN exhibits two flat-spectrum radio sources, J1502SE/SW, offset by 26 mas (140 pc), with each source being energized by its own supermassive black hole (BH). This intriguing interpretation of a close binary BH was reached after ruling out a double-hotspot scenario, wherein both hotspots are energized by a single, central BH, a configuration occurring in the well-studied Compact Symmetric Objects. When observed with sufficient sensitivity and resolution, an object with double hotspots should have an edge-brightened structure. We report evidence from the Very Long Baseline Array (VLBA) for just such a structure in an image of the obscured AGN with higher sensitivity and resolution than the EVN images. We thus conclude that a double-hotspot scenario should be reconsidered as a viable interpretation for J1502SE/SW, and suggest further VLBA tests of that scenario. A double-hotspot scenario could have broad implications for feedback in obscured AGNs. We also report a VLBA detection of high-brightness-temperature emission from the unobscured AGN that is offset several kiloparsecs from J1502SE/SW.

Subject headings: black hole physics — galaxies: active — galaxies: individual (SDSS J150243.09+111557.3) — galaxies: interactions — galaxies: nuclei

¹National Radio Astronomy Observatory, P.O. Box O, Socorro, NM 87801; jwrobel@nrao.edu, cwalker@nrao.edu

²The National Radio Astronomy Observatory (NRAO) is a facility of the National Science Foundation, operated under cooperative agreement by Associated Universities, Inc.

³Department of Physics and Astronomy, University of Iowa, Van Allen Hall, Iowa City, IA 52242, USA; hai-fu@uiowa.edu

1. Motivation

Recent simulations of galaxy mergers are able to produce remnants that contain two or more supermassive black holes (BHs; Hoffman & Loeb 2007; Amaro-Seoane et al. 2010; Kulkarni & Loeb 2012). When such BHs accrete, they can appear as two or more active galactic nuclei (AGNs) on sub-galactic scales (Van Wassenhove et al. 2012; Blecha et al. 2013). Systematic surveys for such multiple AGNs can impose observational constraints on AGN activation and tidally enhanced star formation (e.g., Liu et al. 2012; Koss et al. 2012). Such surveys can also constrain the BH merger rate, a key quantity for predicting the signals expected for pulsar timing arrays and gravity-wave detectors (Hobbs et al. 2010; Dotti et al. 2012; Shannon et al. 2013). These topics are of fundamental importance in astrophysics, so all reports of multiple AGN candidates warrant close vetting (e.g., Wang et al. 2009; Liu et al. 2010; Smith et al. 2010; Fu et al. 2011a, 2012; Comerford et al. 2012; Koss et al. 2012).

This Letter focuses on one such case, SDSS J150243.09+111557.3 (J1502+1115 hereafter), originally identified as a dual AGN candidate at a redshift of $z = 0.39$ with double-peaked profiles of [OIII] (Smith et al. 2010) and later shown to be a merging system with an unobscured, primary AGN, J1502P, offset by $1.4''$ (7.4 kpc)¹ from a dust-obscured, secondary AGN J1502S (Fu et al. 2011b, F11 hereafter). Deane et al. (2014, D14 hereafter) recently advanced J1502S as *itself* hosting two AGNs and, thus, two supermassive BHs. Adding in the AGN J1502P then suggests that the merging system J1502+1115 hosts three supermassive BHs on sub-galactic scales.

Specifically, D14 reported evidence from the European VLBI Network (EVN) that J1502S exhibits two flat-spectrum radio sources, J1502SE/SW, offset by 26 mas (140 pc), with each source being energized by its own supermassive BH. D14 reached this intriguing interpretation of J1502SE/SW as a close binary BH after ruling out a double-hotspot scenario, wherein both hotspots are energized by a single, central BH in one configuration that defines the well-studied Compact Symmetric Objects (CSOs; Peck & Taylor 2000). When observed with sufficient sensitivity and resolution, an object with double hotspots should have an edge-brightened structure. This Letter reports evidence from the Very Long Baseline Array (VLBA; Napier et al. 1994) for just such structure in an image of J1502S with higher sensitivity and resolution than the EVN images. § 2 presents the new VLBA imaging and § 3 explores its implications. A summary and conclusions appear in § 4.

¹ $H_0 = 70 \text{ km s}^{-1} \text{ Mpc}^{-1}$, $\Omega_M = 0.3$, $\Omega_\Lambda = 0.7$

2. VLBA Imaging

J1502+1115 was observed during a 6-hour session with 9 VLBA antennas on 2013 June 29 (UT) under proposal BW102 = 13A-241. The tenth VLBA antenna, at Fort Davis, TX, was unavailable due to equipment malfunction. J1504+1029 was used as a phase and relative amplitude calibrator (Table 1). The switching time between it and J1502+1115 was 180 s, with about a third of the session devoted to J1504+1029. About once per hour, OQ 208 and J1507+1236 were observed. OQ 208 is a compact and slowly-varying source (Wu et al. 2013, and references therein) observed to check the absolute flux density calibration. J1507+1236 (Table 1) is a VLBA calibrator with a well known position that was observed to check the quality of the phase referencing.

A total of 256 MHz per circular polarization centered on $\nu = 4.980$ GHz (5 GHz hereafter) were recorded using the new RDBE/MARK5C wide-band system at 2 Gbps. Every 1 s the VLBA DiFX correlator (Deller et al. 2011) produced 512 contiguous 0.5-MHz channels. About 3.4 hours were accrued on J1502+1115, during which the VLA position for J1502S (F11) was used for pointing and correlation. Correlation parameters were chosen to ensure distortion-free imaging at the position of J1502P, offset by $1.4''$ from J1502S (F11). VLBA system temperatures and gains were recorded for amplitude calibration.

Observations of OQ 208 on 2013 July 1 UT were retrieved from the archive of the Jansky Very Large Array (VLA) (VLA; Perley et al. 2011). Release 4.1 of the Common Astronomy Software Applications (CASA) package (McMullin et al. 2007) was employed to calibrate and edit the data in an automated fashion ². The final edits and imaging were done in the Astronomical Image Processing System (AIPS; Greisen 2003). To best match the VLBA data, the final VLA image of OQ 208 utilized a total bandwidth of 128 MHz per circular polarization centered at $\nu = 5$ GHz. Direct comparison with the primary flux calibrator 3C 286 yielded a VLA flux density of 2.33 ± 0.07 Jy, with the error dominated by an estimated 3% uncertainty in the amplitude scale (Perley & Butler 2013).

AIPS was used for VLBA calibration and imaging. The calibration strategies documented in Appendix C of the AIPS Cookbook were followed, including doing a bandpass calibration and making corrections for the ionosphere and for updated Earth orientation parameters. The phase calibrator J1504+1029 was imaged using standard methods based on multiple iterations of self-calibration and imaging. Its final image was then used to determine the phase and amplitude corrections to apply to all other data. For OQ 208, only the amplitudes were of interest. For J1507+1236, J1502S, and J1502P, the phases enabled

²science.nrao.edu/facilities/vla/data-processing/pipeline

Table 1. VLBA Astrometry and Photometry at 5 GHz

Source	Peak R.A./Decl. (J2000)	Position Error (mas)	Switching Angle ($^{\circ}$)	Integrated Flux Density ^a (μ Jy)
(1)	(2)	(3)	(4)	(5)
J1504+1029 ^b	15 04 24.979782	0.1
	10 29 39.19840	0.1		
J1507+1236 ^{c,d}	15 07 21.758063	0.3	2.23	...
	12 36 29.07573	0.4		
J1502SE ^c	15 02 43.180261	0.2	0.87	891 \pm 81
	11 15 57.06831	0.3		
J1502SW ^c	15 02 43.178473	0.2	0.87	1010 \pm 92
	11 15 57.06508	0.3		
J1502P ^c	15 02 43.088667	0.2	0.87	254 \pm 45
	11 15 57.40016	0.3		

Note. — Col. (1): Source. Col. (2): Position at peak. Units of right ascension are hours, minutes, and seconds, and units of declination are degrees, arcminutes, and arcseconds. Col. (3): Position error. Col. (4): Switching angle to the phase calibrator. Col. (5): Integrated flux density. Error is the quadratic sum of (i) the image rms times the square root of the number of synthesized beam areas integrated over, (ii) a 3% uncertainty due to phase-calibration errors and (iii) a 5% uncertainty in the amplitude scale.

^aMeasured from the images made from self-calibrated data.

^bPhase calibrator. The tabulated position and errors are assumed and adopted from the Petrov catalog rfc_2012b. The latest Petrov catalog is at <http://astrogeo.org/petrov/>.

^cPositions are measured from the images made from phase-referenced data that have not been self-calibrated. The conservative error estimates include measurement errors, systematic phase-referencing errors and the errors in the position of the phase reference calibrator.

^dPhase-referencing check. The astrometric catalog position from Petrov rfc_2014a is R.A.=15 07 21.758075 (\pm 0.13 mas) and Decl. = 12 36 29.07581 (\pm 0.21 mas). It differs from our measured position by 0.18 mas in R.A. and 0.08 mas in Decl.

phase-referenced imaging, and those images were used to measure the positions in Table 1. After exploring various imaging schemes, a robustness of 1 as implemented in AIPS was adopted.

The OQ 208 data were self-calibrated and imaged, yielding an integrated VLBA flux density of 1.78 Jy, 31% lower than the VLA value. This finding corroborated a recent report of low calibrated flux densities from another VLBA user group. The cause is under investigation and seems to affect mainly the Polyphase Filter Bank personality of the RDBE system when the bandpass is calibrated in what is believed to be the proper manner. Meanwhile, for this paper, we have scaled the VLBA amplitudes upward by a factor of 1.31 to align the VLA and VLBA photometry for OQ 208, thereby calibrating the VLBA amplitude scale to an accuracy of about 5%.

The J1507+1236 data were self-calibrated and imaged, after which the peak flux density increased by 78% while the integrated flux density did not change significantly, as expected when the emission is concentrated by the improved phases. Compared to 1502+1115, many fewer observations were made of J1507+1236, and those observations involved a switching angle about 2.5 times larger (Table 1). Thus the quality of the J1502+1115 data is expected to be much higher. From the self-calibrated data for J1504+1029 and J1507+1236, the integrated flux densities are 990 ± 50 mJy and 208 ± 10 mJy, respectively, with errors dominated by the 5% uncertainty in the amplitude scale.

The J1502+1115 data contains information on J1502P and J1502S. D14 did not detect J1502P, whereas our phase-referenced image of it detects one radio source. Our phase-referenced image of J1502S shows that it consists of two radio sources, as reported by D14, with a summed flux density of less than 2 mJy. This image was used to self-calibrate the phases of the J1502+1115 data. Because J1502S is so faint, the phase-only self-calibration was based on data coherently averaged for 35 m over all frequencies and both polarizations. This long coherent average was possible because the initial phase referencing had already removed the short-term phase fluctuations. This phase self-calibration was used to reduce residual systematic calibration offsets. For J1502S, the improved calibration recovered an additional $\sim 10\%$ in the peak flux densities and $\sim 5\%$ in the integrated flux densities. Self-calibration at low signal-to-noise (S/N) can adjust the flux density upwards excessively by gathering noise, or downward by failing to calibrate the residual phase fluctuations. To account for these effects, our experiments with several coherent averages lead us to include an estimate of a 3% uncertainty in the error budget for the integrated flux densities (term (ii) in Table 1).

Figure 1 shows the self-calibrated VLBA image of J1502S. The achieved rms noise is in line with the estimated thermal noise. Figure 1 reveals that J1502S consists of two radio

sources, labeled J1502SW and J1502SE. This image was used for the photometry in Table 1. With adequate S/N, structures as large as about 20 mas could be represented in Figure 1.

J1502P was imaged twice from the J1502+1115 data, once in its phase-referenced form and once in its self-calibrated form. The data used for imaging retained the 0.5-MHz channels from the correlator to prevent bandwidth smearing, and had its phase center shifted by $-1.329''$ in right ascension and $0.330''$ in declination. J1502P was detected as a slightly resolved source in both images, with the self-calibration providing a 9% enhancement in the peak flux density and no change in the integrated flux density. The signal from J1502P did not enter into the self-calibration, so this is an independent check of the quality of that calibration. An elliptical Gaussian fit in the image plane was consistent with J1502P being unresolved with major and minor axes less than 3.5 mas and 1.5 mas, respectively. Since J1502P is so point-like, no image is presented.

3. Implications

3.1. J1502SE/SW

From EVN images at 1.7 and 5 GHz, D14 reported evidence that the dust-obscured AGN exhibits two flat-spectrum radio sources, J1502SE/SW, offset by 26 mas (140 pc), with each source being energized by its own supermassive BH. While intriguing, this interpretation of a close binary BH hole was adopted only after D14 had ruled out a more prosaic double-hotspot scenario. In a double-hotspot scenario both hotspots are energized by a single, central BH. Such a configuration occurs in a well-studied class of radio-selected AGN, the CSOs (An & Baan 2012, and references therein). CSOs have radio extents of less than 1 kpc; slow-moving emission on both sides of the central engine; and weak, if any, radio variability (e.g., Fasnacht & Taylor 2001). When observed with sufficient sensitivity and resolution, the overall structure of a CSO can appear edge-brightened, that is, the emission is brightest at the CSO’s extremities, called hotspots, and becomes fainter closer to its central BH. The radio sources J1502SE/SW were only slightly resolved in the EVN images, making it difficult to look for edge-brightening. However, the VLBA image in Figure 1 clearly shows the expected edge-brightened structure for J1502SE/SW. For this reason, we conclude that the double-hotspot scenario should be reconsidered as a viable interpretation for J1502SE/SW.

When compared to CSOs in the compilation of An & Baan (2012), D14 noted that J1502SE/SW has several unusual properties, including an atypically low spectral power of $P_{1.7 \text{ GHz}} = 7 \times 10^{23} \text{ W Hz}^{-1}$ and an atypically flat spectral index of $\alpha_{5 \text{ GHz}}^{1.7 \text{ GHz}} \sim -0.1 \pm 0.1$, especially given its projected linear size. These properties provide important clues as to

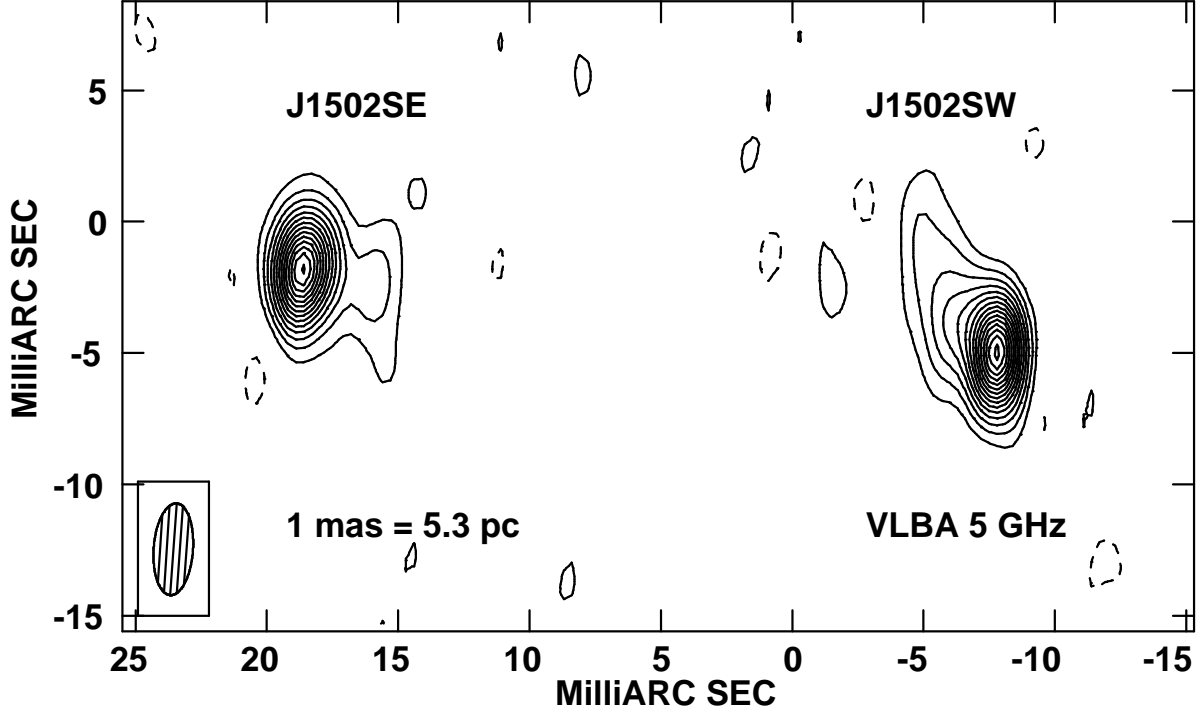


Fig. 1.— VLBA image of Stokes I emission from the dust-obscured AGN J1502S at $\nu = 5$ GHz after self calibration. The rms noise is $\sigma = 21 \mu\text{Jy beam}^{-1}$ and the synthesized beam dimensions at FWHM are $3.5 \text{ mas} \times 1.5 \text{ mas}$ with an elongation position angle $\text{PA} = -4^\circ$ (boxed hatched ellipse). Allowed contours are at $-6, -4, -2, 2, 4, 6, 8, 10, \dots$ and 30 times 1σ . Negative contours are dashed and positive ones are solid. The coordinate origin is at the VLA position for J1502S (F11). Clear edge-brightening is observed, suggesting that the two sources are hotspots energized by a single, centrally-located BH. The western extension of J1502SE has a peak of 5.7σ .

the nature of J1502SW/SE. Below, we discuss these properties within an alternate, and yet related, context that stems from two findings for AGNs with radio powers similar to J1502SE/SW.

First, the radio source J1148+5924 has a spectral power of $P_{1.4 \text{ GHz}} \sim 2 \times 10^{23} \text{ W Hz}^{-1}$, a factor of a few below that of J1502S (Taylor et al. 1998). J1148+5924 is dominated by radio emission with an extent of less than 1 kpc, shows a slow apparent separation speed of 0.3c on parsec scales, and displays slow radio variability (Taylor et al. 1998; Peck & Taylor 2000; Fassnacht & Taylor 2001). Such traits are shared by the powerful CSOs (An & Baan 2012), suggesting that J1148+5924 is a low-power CSO. Moreover, J1502S shows evidence for an overall rotational symmetry on scales 0.1-10 kpc (D14). J1148+5924 also shows evidence for an overall rotational symmetry on similar scales, possibly caused by interactions between the low-power radio outflow and the circumnuclear gas and dust (Wrobel & Heeschen 1984; Taylor et al. 1998; Perlman et al. 2001). Redshifted HI is seen in absorption against the two-sided structures in J1148+5924 (Peck & Taylor 1998), and this infalling gas could fuel and/or distort the slow-moving radio outflow.

Second, the obscured AGN J1502S was originally [OIII]-selected (Smith et al. 2010) and has a luminosity of $L([\text{OIII}]) = 3.6 \times 10^{42} \text{ erg s}^{-1}$. In their analysis of the radio properties of obscured AGN that have $L([\text{OIII}]) \sim 10^{42} \text{ erg s}^{-1}$, Lal & Ho (2010) find a high incidence of spectra that are flat or rising between 1.4 and 8.4 GHz. Those authors speculate that such radio spectra could be caused by free-free absorption in the ionized gas traced in [OIII]. J1502S has a similar [OIII] luminosity. This hints that free-free absorption could contribute to the flat spectra D14 measure for J1502SE/SW, although achieving flatness between 1.7-15.7 GHz could be a challenge for such an absorption model. Still, this suggestion is testable with VLBA imaging spanning a wide frequency range (e.g., Marr et al. 2014), which could also help reveal emission from a centrally located origin of activity.

D14 cite a 10% uncertainty in the amplitude scale of the EVN at 5 GHz. Factoring this into their reported photometry leads to flux densities of $857 \pm 99 \mu\text{Jy}$ and $872 \pm 100 \mu\text{Jy}$ for J1502SE and J1502SW, respectively, in 2011 April 12. Comparison with the VLBA photometry (Table 1) obtained more than two years later implies no time variability, another trait consistent with CSO-like behavior. From the EVN images, the apparent separation between J1502SE and J1502SW increases by less than 5 pc yr^{-1} . For comparison, for J1148+5924 the apparent separation increases by 0.1 pc yr^{-1} . If J1502SE/SW have a similarly-slow apparent separation, it would be advantageous to monitor that separation with the VLBA’s higher sensitivity and higher resolution.

More broadly, establishing a double-hotspot scenario for the dust-obscured AGN J1502S could have important implications for feedback in obscured AGNs, whether those AGN are

discovered in surveys for X-ray or infrared continuum or for narrow optical emission lines (Lal & Ho 2010, and references therein) or in increasingly deep VLBA surveys (Middelberg et al. 2013; Deller & Middelberg 2014, and references therein). Conversely, our study underscores the importance of culling double-hotspot sources from VLBA surveys seeking candidate binary BHs on parsec scales (e.g., Burke-Spolaor 2011; Tingay & Wayth 2011) or strong gravitational lenses on mas scales (Wilkinson et al. 2001).

3.2. J1502P

From Table 1 the VLBA detection of J1502P at $\nu = 5$ GHz has a rest-frame brightness temperature of 4.8 million K, or more if truly unresolved. Such levels are not achieved by even the most compact starbursts (Condon 1992). Also, the VLBA image is too shallow to detect even the most luminous radio supernovae beyond $z \sim 0.1$ (e.g., Middelberg et al. 2013). Thus the VLBA detection indicates that J1502P must be AGN driven, confirming, independent of F11, that J1502P hosts an AGN. At $\nu = 5$ GHz, the VLA photometry (F11) localizes the emission to a diameter of 300 mas (1.6 kpc), whereas the EVN photometry (D14), obtained only about two months earlier, recovers less than 20% of the VLA signal. Both this fact and the overall steep-spectrum nature of J1502P (F11) suggest that source-resolution effects are at play, a motivation for deeper VLBA imaging.

4. Summary and Conclusions

We used the VLBA at 5 GHz to image J1502+1115, a merging system at $z = 0.39$ containing a dust-obscured AGN, J1502S, offset by $1.4''$ (7.4 kpc) from an unobscured AGN, J1502P (F11).

Regarding J1502S, D14 advocate it as hosting two AGNs and, thus, two supermassive BHs, based on EVN images at 1.7 and 5 GHz showing two slightly-resolved, flat-spectrum radio sources, J1502SE/SW, offset by 26 mas (140 pc). D14 reached their intriguing interpretation of a 140-pc binary BH after discounting a double-hotspot scenario, wherein both hotspots are energized by a single, central BH, a configuration occurring amongst radio-selected CSOs. When observed with sufficient sensitivity and resolution, an object with double hotspots should have an edge-brightened appearance. We find clear evidence for such edge-brightening in our VLBA image of J1502S that has higher sensitivity and resolution than the EVN images. We thus conclude that the double-hotspot scenario should be reconsidered as a viable interpretation for J1502SE/SW. We also suggest that free-free absorption

by J1502S’s [OIII] emitting gas could help flatten the radio spectra of J1502SE/SW. Future VLBA imaging can further test the double-hotspot scenario for J1502SE/SW, as well as the potential role of free-free absorption. A double-hotspot scenario could have important consequences for feedback modes in obscured AGNs, a key population for understanding evolutionary linkages between galaxies and the BHs they host. Future VLBA imaging of samples of low-power CSOs is also needed to investigate trends between spectral indices and projected linear sizes, to help distinguish low-power CSOs from close binary BHs. And because the detection of polarized intensity is relatively rare among powerful CSOs (Helmboldt et al. 2007), such VLBA imaging should include polarimetry as a possible discriminant between low-power CSOs and close binary BHs.

Regarding J1502P, as it is detected in our VLBA image, it must be AGN driven. This confirms, independent of F11, that J1502P hosts an AGN. The VLBA detection is faint, only $254\ \mu\text{Jy}$. Future, deeper VLBA imaging is needed to characterize it further.

We thank the anonymous referee and the commentator, Roger Deane, for prompt and helpful feedback. This work made use of the Swinburne University of Technology software correlator, developed as part of the Australian Major National Research Facilities Programme and operated under licence. We acknowledge using Ned Wright’s Cosmology Calculator (Wright 2006). We are grateful to Drew Medlin for providing only the calibrator scans from the VLA data archived on 2013 July 1.

Facilities: VLA, VLBA.

REFERENCES

- An, T., & Baan, W.A., 2012, ApJ, 760, 77
- Amaro-Seoane, P., Sesana, A., Hoffman, L., et al. 2010, MNRAS, 402, 2308
- Blecha, L., Loeb, A., & Narayan, R. 2013b, MNRAS, 429, 2594
- Burke-Spolaor, S. 2011, MNRAS, 410, 2113
- Comerford, J.M., Gerke, B.F., Stern, D., et al. 2012, ApJ, 753, 42
- Condon, J.J. 1992, ARA&A, 30, 575
- Deane, R.P., Paragi, Z., Jarvis, M.J., et al. 2014, Nature, 511, 57 (D14)
- Deller, A.T., Briske, W.F., Phillips, C.J., et al. 2011, PASP, 123, 275

- Deller, A.T., & Middelberg, E. 2014, *AJ*, 147, 14
- Dotti, M., Sesana, A., & Decarli, R. 2012, *Advances in Astronomy*, 940568
- Fassnacht, C.D., & Taylor, G.B. 2001, *AJ*, 122, 1661
- Fu, H., Myers, A.D., Djorgovski, S.G., & Lin, Y. 2011a, *ApJ*, 733, 103
- Fu, H., Zhang, Z., Assef, R.J., et al. 2011b, *ApJ*, 740, L44 (F11)
- Fu, H., Lin, Y., Myers, A.D., et al. 2012, *ApJ*, 745, 67
- Greisen, E.W. 2003, in *Information Handling in Astronomy*, ed. A. Heck (Dordrecht: Kluwer), 109
- Guedes, J., Madau, P., Mayer, L., & Callegari, S. 2011, *ApJ*, 729, 125
- Helmboldt, J.F., Taylor, G.B., Tremblay, S., et al. 2007, *ApJ*, 658, 203
- Hobbs, G., Archibald, A., Arzoumanian, Z., et al. 2010, *Class. Quantum Grav.*, 27, 084013
- Hoffman, L. & Loeb, A. 2007, *MNRAS*, 377, 957
- Koss, M., Mushotzky, R., Teiester, et al. 2012, *ApJ*, 746, L22
- Kulkarni, G. & Loeb, A. 2012, *MNRAS*, 422, 1306
- Lal, D.V., & Ho, L.C. 2010, *AJ*, 139, 1089
- Liu, X., Shen, Y., Strauss, M.A., & Greene, J.E. 2010, *ApJ*, 708, 427
- Liu, X., Shen, Y., & Strauss, M.A. 2012, *ApJ*, 745, 94
- Marr, J.M., Perry, T.M., Read, J., Taylor, G.B., & Morris, A.O. 2014, *ApJ*, 780, 178
- McMullin, J. P., Waters, B., Schiebel, D., Young, W., & Golap, K. 2007, *Astronomical Data Analysis Software and Systems XVI (ASP Conf. Ser. 376)*, ed. R. A. Shaw, F. Hill, & D. J. Bell (San Francisco, CA: ASP), 127
- Middelberg, E., et al. 2013, *A&A*, 551, A97
- Napier, P.J., Bagri, D.S., Clark, B.G., et al. 1994, *Proc. IEEE*, 82, 658
- Peck, A.B., & Taylor, G.B. 1998, *ApJ*, 502, L23
- Peck, A.B., & Taylor, G.B. 2000, *ApJ*, 534, 90

- Perlman, E.S., Stocke, J.T., Conway, J., & Reynolds, C. 2001, *ApJ*, 122, 536
- Perley, R. A., Chandler, C. J., Butler, B. J., & Wrobel, J. M. 2011, *ApJ*, 739, L1
- Perley, R.A., & Butler, B.J. 2013, *ApJS*, 204, 19
- Shannon, R.M., et al. 2013, *Science*, 342, 334
- Shen, Y., Liu, X., Greene, J.E., & Strauss, M.A. 2011, *ApJ*, 735, 48
- Smith, K.L., Shields, G.A., Bonning, E.W., et al. 2011, *ApJ*, 716, 866
- Taylor, G.B., Wrobel, J.M., & Vermeulen, R.C. 1998, *ApJ*, 498, 619
- Tingay, S.J., & Wayth, R.B. 2011, *AJ*, 141, 174
- Van Wassenhove, S., Volonteri, M., Mayer, L., et al. 2012, *ApJ*, 748, L7
- Wang, J., Chen, Y., Hu, C., Mao, W., & Bian, W. 2009, *ApJ*, 705, L76
- Wrobel, J.M., & Heeschen, D.S. 1984, *ApJ*, 287, 41
- Wilkinson, P.N., Henstock, D.R., Browne, I.W.A., et al. 2001, *Phys. Rev. Lett.*, 86, 584
- Wright, E.L. 2006, *PASP*, 118, 1711
- Wu, F., et al. 2013, *A&A*, 550, A113